

Neutron study of magnetic-moment distribution in Ni-Pt alloys

R. E. Parra* and J. W. Cable

Solid State Division, Oak Ridge National Laboratory, Oak Ridge, Tennessee 37830

(Received 26 November 1979)

The average moments and the moment disturbances of ferromagnetic Ni-Pt alloys with concentrations of 20, 30, 40, 50, 55, and 57 at. % Pt have been measured by the magnetic diffuse scattering of neutrons. The data have been analyzed with the linear superposition model of Marshall including short-range order. The data have also been discussed in terms of Medina's chemical-magnetic environment model which assumes that the moment on an Ni atom is a function of the magnetic moments of the surrounding atoms and of its nearest chemical environment. The results show that the average Ni moment decreases with increasing Pt concentration, while Pt has an average moment of about half that of Ni. The moment disturbance functions, corrected for short-range order, show peaks in the forward direction corresponding to inhomogeneous-moment distributions which may be described as ferromagnetic clusters. The analysis of the data with the chemical-magnetic environment model shows that most of the moment disturbances are caused by the magnetic environment in accordance with other Ni-based alloys. An apparent difference in the macroscopic magnetization of these systems is attributed to differences in chemical short-range order rather than to a different mechanism for the onset of ferromagnetism.

I. INTRODUCTION

The magnetic properties of ferromagnetic Ni-Pt alloys have long been analyzed in terms of the Stoner¹ and Edwards-Wohlfarth² models of itinerant ferromagnetism. Such treatments were based on extensive investigations³⁻⁵ of the bulk magnetic properties of these alloys which, using the Landau theory of phase transitions, provided evidence of an apparent homogeneity of the spatial distribution of the magnetic moments in this system. Some difficulties, however, have been encountered in applying the Stoner-Edwards-Wohlfarth (SEW) model to weak ferromagnets such as Ni-Pt. In particular, the experimental variation of the magnetization at zero field and zero temperature M_{00} and of the Curie temperature T_c with the concentration and the pressure does not agree with the predictions of the SEW model.⁶

A spatially homogeneous-moment distribution in Ni-Pt alloys is in sharp contrast to the behavior of other Ni-based systems such as Ni-Cu (Refs. 7-9) and Ni-Rh (Refs. 10 and 11), which exhibit distinctly inhomogeneous-moment distributions in the form of ferromagnetic clusters near the critical concentration (c_0). Neutron results⁹ have shown that the state of chemical order plays an important role in the determination of the moment distribution in the NiCu system. The magnetic behavior of Ni-Pt also shows a dependence on its chemical order³: The equiatomic alloy is ferromagnetic when atomically disordered and paramagnetic when atomically ordered suggesting that the moment on an Ni atom is dependent on the number of Ni nearest neighbors. However, magnetization measurements indicate magnetic clus-

ters in Ni-Cu but not in Ni-Pt.

An experimental microscopic characterization of the moment distribution in NiPt would help to better understand this system. We therefore decided to measure the magnetic moments and moment disturbances of this system by neutron diffuse scattering. The data were analyzed with the Marshall¹² model of linear superposition of moment perturbations and with a local environment model of Medina and Cable.⁹

II. CROSS SECTIONS AND CORRELATIONS

Diffuse scattering cross sections were measured by both the polarized and the unpolarized neutron methods.^{9,13} It has been shown⁹ that, in the absence of lattice distortions, the cross section per atom for diffuse scattering of polarized neutrons from a binary alloy is

$$d\sigma^{\pm}/d\Omega = c(1-c)[(\Delta b)^2 S(\vec{k}) \pm (0.54)\Delta b \mathcal{M}(\vec{k}) + (0.27)^2 T(\vec{k})], \quad (2.1)$$

where (\pm) denotes the neutron polarization with respect to the direction of the applied field, Δb is the difference between the nuclear scattering amplitudes b_i and b_h of impurity and host atoms, and c is the impurity concentration. $S(\vec{k})$ is the nuclear scattering function expressed in terms of Cowley short-range order (SRO) parameters $\alpha(\vec{R})$,

$$S(\vec{k}) = \sum_{\vec{R}} \alpha(\vec{R}) e^{i\vec{k}\cdot\vec{R}}, \quad (2.2)$$

$T(\vec{k})$ is a moment-moment correlation written as a function of the moment $\mu_{\vec{n}}$ at site \vec{n} and its form factor $f_{\vec{n}}(\vec{k})$,

$$\mu_{\bar{n}}(\bar{\mathbf{K}}) = \mu_{\bar{n}} f_{\bar{n}}(\bar{\mathbf{K}}), \quad (2.3)$$

$$c(1-c)T(\bar{\mathbf{K}}) = \sum_{\bar{\mathbf{R}}} e^{i\bar{\mathbf{R}} \cdot \bar{\mathbf{K}}} \langle [\mu_{\bar{n}+\bar{\mathbf{R}}}(\bar{\mathbf{K}}) - \langle \mu(\bar{\mathbf{K}}) \rangle] \times [\mu_{\bar{n}}(\bar{\mathbf{K}}) - \langle \mu(\bar{\mathbf{K}}) \rangle] \rangle, \quad (2.4)$$

and $\mathfrak{M}(K)$ is a site-occupation-magnetic-moment correlation function given by

$$c(1-c)\mathfrak{M}(\bar{\mathbf{K}}) = \sum_{\bar{\mathbf{R}}} e^{i\bar{\mathbf{R}} \cdot \bar{\mathbf{K}}} \langle (p_{\bar{n}+\bar{\mathbf{R}}} - c)[\mu_{\bar{n}}(\bar{\mathbf{K}}) - \langle \mu(\bar{\mathbf{K}}) \rangle] \rangle, \quad (2.5)$$

where $p_{\bar{n}}$ is a site occupation operator which is unity if there is an impurity at \bar{n} and zero otherwise. The SRO parameters are expressed in terms of these operators by the equation

$$c(1-c)\alpha(\bar{\mathbf{R}}) = \langle (p_{\bar{n}+\bar{\mathbf{R}}} - c)(p_{\bar{n}} - c) \rangle. \quad (2.6)$$

Using Marshall's model,¹² Medina and Cable⁹ have proved that in the presence of SRO $\mathfrak{M}(\bar{\mathbf{K}})$ can be written in terms of $S(\bar{\mathbf{K}})$ by the equation

$$\mathfrak{M}(\bar{\mathbf{K}}) = S(\bar{\mathbf{K}})M(\bar{\mathbf{K}}), \quad (2.7)$$

where $M(K)$ is approximately the random-alloy moment response to a concentration fluctuation:

$$M(\bar{\mathbf{K}}) = \mu_i f_i(\bar{\mathbf{K}}) - \mu_h f_h(\bar{\mathbf{K}}) + (1-c)G(\bar{\mathbf{K}})f_h(\bar{\mathbf{K}}) + cH(\bar{\mathbf{K}})f_i(\bar{\mathbf{K}}). \quad (2.8)$$

Here $G(\bar{\mathbf{K}})$ and $H(\bar{\mathbf{K}})$ are Fourier transforms of the impurity-induced moment disturbances at the host and impurity sites, respectively. Marshall gives the following expression for $T(\bar{\mathbf{K}})$:

$$T(\bar{\mathbf{K}}) = S(\bar{\mathbf{K}})M(\bar{\mathbf{K}})^2 + \dots, \quad (2.9)$$

where the dots indicate small nonlinear terms which are increasingly negligible.

The difference in size of Ni and Pt atoms suggests the appearance of lattice displacements δ^{ij} which are dependent on the type of atoms making up the pair and which produce small contributions to the diffuse scattering.^{14,15} In the presence of lattice displacements (LD) additional $\bar{\mathbf{K}}$ -dependent terms appear in the cross sections and $S(\bar{\mathbf{K}})$ in Eq. (2.1) should be replaced by

$$S(\bar{\mathbf{K}}) + D(\bar{\mathbf{K}})/\Delta b \quad (2.10)$$

and $\mathfrak{M}(\bar{\mathbf{K}})$ by

$$\mathfrak{M}(\bar{\mathbf{K}}) + B(\bar{\mathbf{K}})/\Delta b, \quad (2.11)$$

where $D(\bar{\mathbf{K}})$ and $B(\bar{\mathbf{K}})$ are lattice-displacement scattering functions given by

$$D(\bar{\mathbf{K}}) = \sum_{\bar{\mathbf{R}}} e^{i\bar{\mathbf{R}} \cdot \bar{\mathbf{K}}} \bar{\mathbf{K}} \cdot \left[\left(\frac{c}{1-c} + \alpha(\bar{\mathbf{R}}) \right) b_i \bar{\delta}^{ii} - \left(\frac{1-c}{c} + \alpha(\bar{\mathbf{R}}) \right) b_h \bar{\delta}^{hh} \right], \quad (2.12)$$

$$B(\bar{\mathbf{K}}) = \frac{1}{2} \sum_{\bar{\mathbf{R}}} e^{i\bar{\mathbf{R}} \cdot \bar{\mathbf{K}}} \bar{\mathbf{K}} \cdot \left[\left(\frac{c}{1-c} + \alpha(\bar{\mathbf{R}}) \right) \bar{\delta}^{ii} (b_i \Delta \mu + \mu_i \Delta b) - \left(\frac{1-c}{c} + \alpha(\bar{\mathbf{R}}) \right) \bar{\delta}^{hh} (\mu_h \Delta b + b_h \Delta \mu) \right]. \quad (2.13)$$

Polycrystalline samples give spherically averaged cross sections which are denoted in the correlation functions by dropping the vector symbol on $\bar{\mathbf{K}}$. The spherical average of $S(\bar{\mathbf{K}})$ and $D(\bar{\mathbf{K}})$ gives the SRO and LD parameters while that of $\mathfrak{M}(\bar{\mathbf{K}})$ gives

$$\mathfrak{M}(K) = \langle \mu_i(K) \rangle - \langle \mu_h(K) \rangle + \dots, \quad (2.14)$$

where $\langle \mu_i(K) \rangle$ and $\langle \mu_h(K) \rangle$ are the average impurity and host moments and the dots indicate decaying oscillatory terms.

With unpolarized neutrons the nuclear-magnetic cross term in Eq. (2.1) vanishes leaving only the purely nuclear and purely magnetic terms. The contribution of the magnetic term to the cross section depends on the moment orientation relative to the scattering vector, and this dependence is used to separate the nuclear and magnetic scattering in the well-established field-off minus field-on method.

III. EXPERIMENTAL PROCEDURES

Ferromagnetic samples of ⁶⁰Ni-Pt with 20, 30, 40, 50, 55, and 57 at. % Pt were prepared by arc melting and drop casting. X-ray analysis gave the following lattice parameters: 20, at. % Pt sample, $a = 3.6274 \text{ \AA}$; 30, $a = 3.6716 \text{ \AA}$, 40, $a = 3.7135 \text{ \AA}$; 50, $a = 3.7535 \text{ \AA}$, 55, $a = 3.7713 \text{ \AA}$; 57, $a = 3.7803 \text{ \AA}$. Neutron samples were cut from the cast ingots and machined into flat polycrystalline plates. Small pillar-shaped specimens were cut from the neutron samples for the magnetization measurements. The samples were annealed at 1000 °C for 24 h and then quenched.

The neutron experiments were carried out at the Oak Ridge National Laboratory. The polarized neutron measurements were made at the High Flux Isotope Reactor (HFIR) and the unpolarized neutron cross sections were measured at the Oak Ridge Research Reactor (ORR). A monochromatic beam of wavelength $\lambda = 1.067 \text{ \AA}$ was obtained at the HFIR from an FeSi monochromator which serves also as a neutron polarizer. The samples were

set in symmetric transmission geometry and held at 4.2 K. Superconducting coils produced a vertical magnetic field that was applied to the sample. The measurements were made with a field of 40 kOe. For the 50, 55, and 57 at. % Pt samples additional measurements were made at a neutron wavelength of 1.216 Å, the longer wavelength being used to achieve smaller K values. Absolute cross sections were obtained by calibration with a vanadium sample. Measurements were made with neutrons polarized parallel and antiparallel to the magnetic field and were corrected for (1) beam attenuation and instrumental background, (2) incomplete incident polarization and flipper efficiency, (3) depolarization of the beam, (4) thermal diffuse scattering, (5) incoherent scattering, and (6) multiple Bragg scattering.

The measurements at the ORR were made with long-wavelength 4.43-Å neutrons and with the samples at a temperature of 10 K. Two sets of measurements were carried out, one with a field of 10 kOe parallel to the scattering vector and the other with no field at all. The cross sections were calibrated with a standard V scatterer.

As the critical concentration is approached the magnetic moments become more dependent on concentration and SRO and, since the latter may be sample dependent to a certain extent, we decided to measure the magnetizations of our samples. The magnetizations of the small pillar-shaped specimens were measured with the extraction method at 4.2 K. The measurements were calibrated with an Ni sample assuming an Ni moment of $0.616\mu_B/\text{atom}$.

IV. EXPERIMENTAL RESULTS

Nuclear scattering functions were obtained from both the polarized and unpolarized neutron data. This is readily accomplished with the unpolarized neutron data for which the field-on cross sections, after correction for instrumental background, contain only incoherent and nuclear disorder scattering. The incoherent scattering is due mainly to the Pt atoms since we are using isotopic Ni and, to subtract this part of the scattering, we

measured the incoherent cross section of pure Pt under the same experimental conditions. The value obtained was $(d\sigma/d\Omega)_{\text{inc}} = 32 \pm 3$ $\text{mb sr}^{-1} \text{atom}^{-1}$. These data only cover the range $0.2 < K < 1.25 \text{ \AA}^{-1}$ and must be combined with the polarized neutron data to describe the SRO of these samples. With polarized neutrons, the sum of the spin-up and spin-down cross sections contains not only the desired nuclear disorder scattering but also contributions due to incoherent, multiple, magnetic disorder, and thermal diffuse scattering. The last two contributions are small and calculable and were directly subtracted. The remaining incoherent and multiple scattering was retained in the sum cross sections. This was assumed to be isotropic with a magnitude that was left as a fitting parameter in the first analysis. The fitted parameter was then subtracted to obtain the nuclear disorder scattering. The resulting $S(K)$ functions were found to agree within experimental error with the unpolarized results in the overlap region. The combined data were least-squares fitted with the spherical average of Eq. (2.2) as modified by Eq. (2.10) to include lattice distortions,

$$S(K) = \sum_j z_j \alpha(R_j) \frac{\sin KR_j}{KR_j} + \sum_j z_j \beta(R_j) \left(\frac{\sin KR_j}{KR_j} - \cos KR_j \right), \quad (4.1)$$

where z_j is the coordination number of the shell of radius R_j and the fitting parameters are α for SRO and β for LD. The results of the fitting are given in Fig. 1 and the fitted parameters are given in Table I. Theoretically $\alpha(0) = 1$ but this was left as a free parameter to compensate for any error in the determination of the incoherent and multiple-scattering contributions that were subtracted. The SRO parameters are large and extend to several shells, corresponding to a large amount of SRO. They tend to alternate in sign as expected for the type of ordered configurations (Cu_3Au and CuAu) that develop in these alloys; the negative first-neighbor parameter corresponds to a higher

TABLE I. Short-range order and lattice displacement parameters for Ni-Pt alloys.

c	α_0	α_1	α_2	α_3	α_4	α_5	β_1	χ^2/N
0.2	1.019(12)	-0.138(5)	0.098(20)	0.041	-0.073	0.004	-0.033(4)	0.96
0.3	1.049(12)	-0.160(5)	0.191(19)	0.017	-0.042	-0.002	-0.043(4)	1.59
0.4	1.036(11)	-0.159(5)	0.215(19)	-0.006	-0.004	-0.007	-0.050(4)	1.68
0.5	0.963(10)	-0.135(5)	0.226(18)	-0.043	0.075	0.019	-0.057(4)	1.37
0.55	1.180(12)	-0.167(5)	0.294(23)	-0.069	0.138	0.037	-0.071(5)	1.37
0.57	1.044(10)	-0.122(5)	0.178(20)	-0.041	0.095	0.025	-0.067(4)	1.98

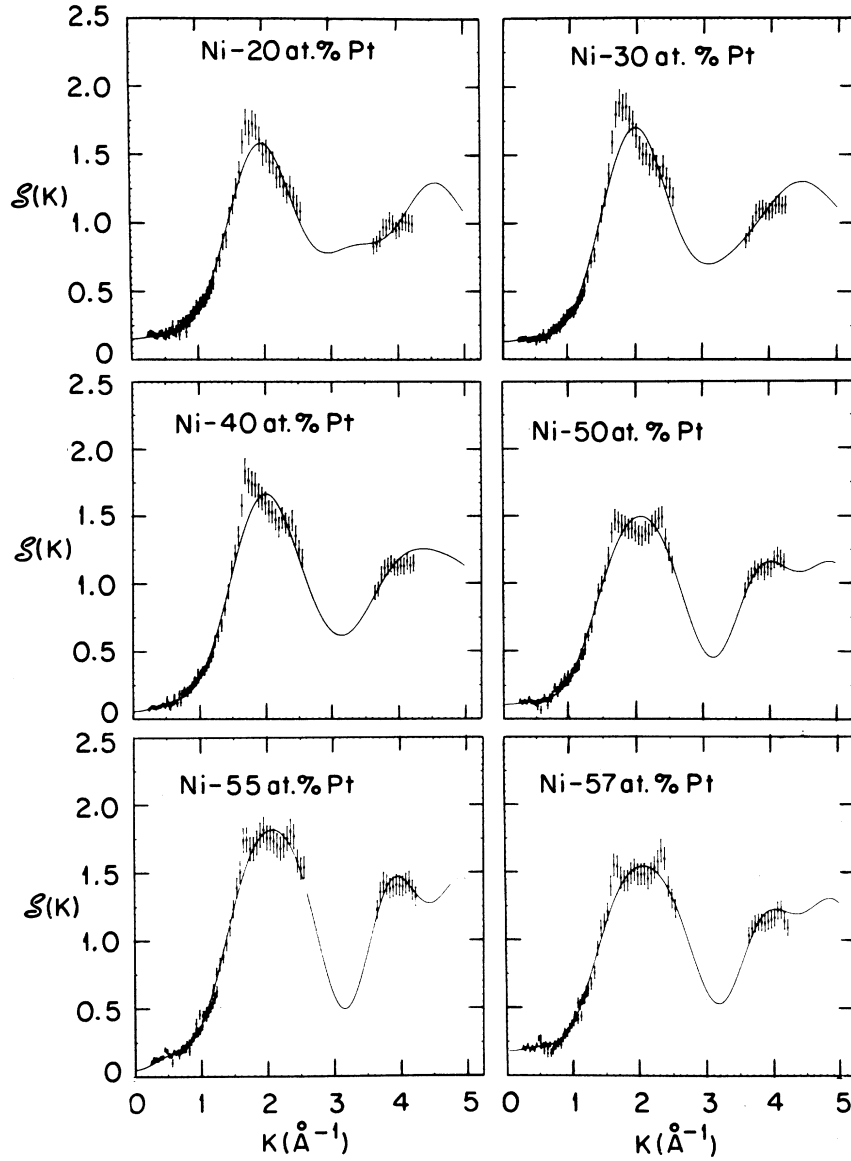


FIG. 1. Nuclear diffuse scattering functions for NiPt. Bragg peaks occur in those regions where no data points are shown. The overlapping unpolarized and polarized-neutron data in the $0.5\text{--}1.25\text{ \AA}^{-1}$ region confirms the incoherent and multiple Bragg-correction procedure described in the text.

than random probability of Pt atoms as nearest neighbors of Ni atoms.

Lattice displacements are typically very small and only the nearest neighbors need to be considered. The LD parameters yield the value $\delta = 0.077(3)\text{ \AA}$, where $\delta = \lim_{c \rightarrow 0} \delta^{ii}$. The positive δ corresponds to an expansion of the lattice around the large Pt atoms. These static displacements agree with radial displacements calculated for fcc systems using elastic constants and lattice parameter data.¹⁶

The only significant corrections to the difference of the spin-up and spin-down cross sections are

due to the incomplete incident polarization and spin reversal. These are readily calculable and amount to approximately 10% of the observed difference signal. The nuclear-magnetic correlation functions $\mathfrak{M}(K)$ are obtained from these difference cross sections by use of Eq. (2.1). These have been fitted to the spherical average of Eq. (2.7) which is an equation of the form

$$\mathfrak{M}(K) = \bar{\mu}_{\text{Pt}} f_{\text{Pt}}(K) - \bar{\mu}_{\text{Ni}} f_{\text{Ni}}(K) + \sum_{j=1}^N z_j m_j \frac{\sin KR_j}{KR_j}, \quad (4.2)$$

TABLE II. Moment disturbance parameters of Ni-Pt alloys.

c	$\bar{\mu}_{\text{Ni}}$	$\bar{\mu}_{\text{Pt}}$	k	ϕ_1	$\bar{\mu}_{\text{neutron}}$	$\bar{\mu}_{\text{magn}}$
0.2	0.515(28)	0.276(33)	0.81(13)	-0.028(3)	0.465(23)	0.482(24)
0.3	0.443(22)	0.228(26)	0.43(17)	-0.025(5)	0.381(17)	0.381(19)
0.4	0.373(19)	0.195(23)	0.34(14)	-0.025(4)	0.301(15)	0.285(14)
0.5	0.279(18)	0.170(22)	0.20(3)	-0.016(2)	0.224(14)	0.185(9)
0.55	0.152(18)	0.057(22)	0.16(3)	-0.013(1)	0.100(15)	0.103(5)
0.57	0.145(18)	0.079(22)	0.10(2)	-0.005(1)	0.107(15)	0.078(4)

where the small lattice displacement corrections were neglected and where z_j and R_j have the same meaning as in Eq. (4.1) while the m_j are moment disturbance parameters that include SRO effects. We use $f_{\text{Ni}}(K) = \exp(-0.044 K^2)$ and $f_{\text{Pt}}(K) = \exp(-0.105 K^2)$ which closely approximate the experimental form factors^{17,18} over this limited K region. The difference between the Ni and Pt form factors allows a direct determination of $\bar{\mu}_{\text{Ni}}$ and $\bar{\mu}_{\text{Pt}}$ as fitting parameters. The moments obtained are given in Table II and are shown in Fig. 2 where the quoted errors are the statistical errors from the fitting. Both moments decrease continuously with increasing Pt concentration with the Pt moment about one-half that of Ni. These individual moments yield average moments that are compared in Fig. 3 with those obtained from our bulk magnetization data. The agreement is very good. The fitted $\mathfrak{M}(K)$ curves are shown in Fig. 4. The unmodulated level of these functions at large K is just the difference between the average Ni and Pt moments. Aside from these differences these functions show very little structure corresponding to fairly homogeneous-moment distributions in the alloys with chemical SRO.

The effects of SRO on the moment distribution can be removed by simply dividing $\mathfrak{M}(K)$ by $S(K)$

[see Eq. (2.7)]. The resulting $M(K)$ data, which are displayed in Fig. 5, are then fitted with the spherical average of the function given by Eq. (2.8). Since $G(K)$ and $H(K)$ have the same form, the individual Ni and Pt moment disturbances cannot be separately determined. We therefore define a new function as the weighted sum of these two disturbance functions

$$cH(K)f_{\text{Pt}}(K) + (1-c)G(K)f_{\text{Ni}}(K) = \sum_i z_i \phi_i \frac{\sin KR_i}{KR_i}, \quad (4.3)$$

and fit $M(K)$ with

$$M(K) = \Delta\mu(K) + \sum_i z_i \phi_i \frac{\sin KR_i}{KR_i} + \sum_i z_i \gamma_i \left(\frac{\sin KR_i}{KR_i} - \cos KR_i \right), \quad (4.4)$$

where ϕ_i and γ_i are the moment disturbance and lattice displacement parameters. We assume a Yukawa form¹⁹ for ϕ_i , i.e.,

$$\phi_i = (R_1/R_i)\phi_1 \exp[-k(R_i - R_1)], \quad (4.5)$$

and use k as an additional parameter of the fitting

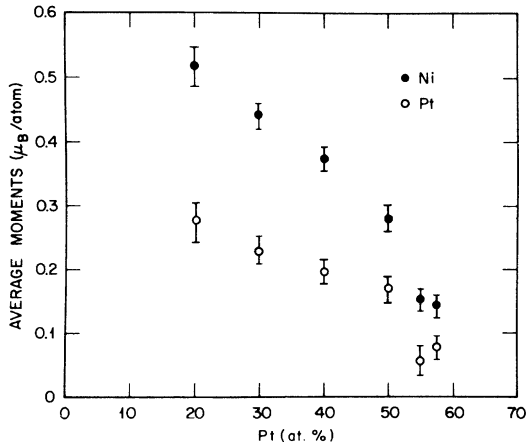


FIG. 2. Average individual moments of NiPt.

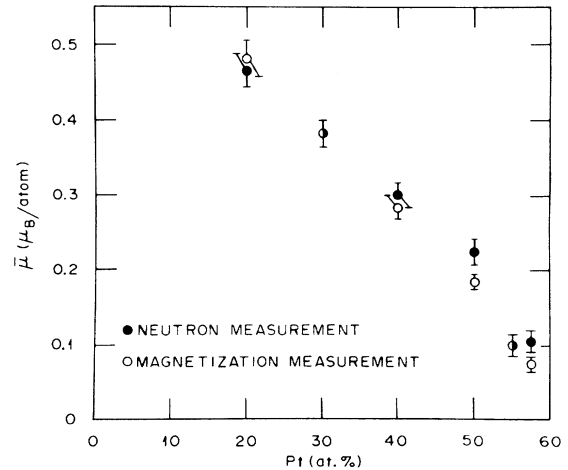


FIG. 3. Comparison of NiPt average moments from neutron and magnetization measurements.

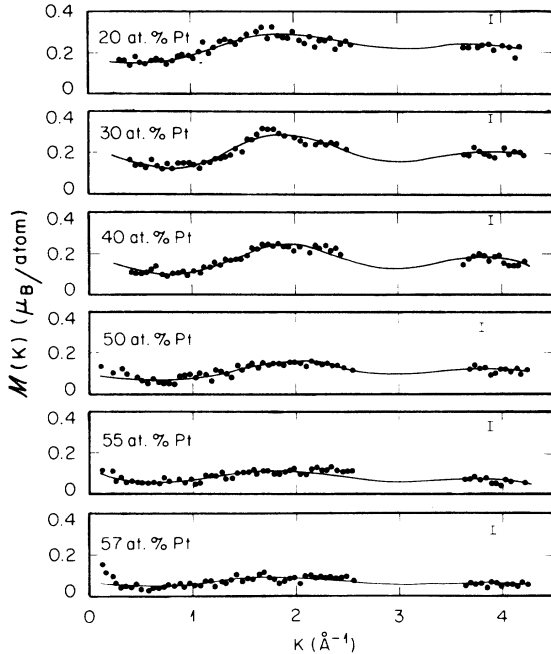


FIG. 4. Nuclear-magnetic correlation functions for NiPt.

to describe the radial extent of the moment disturbances. This gives a good description of the data as shown in Fig. 5. The arrows indicate values of $d\bar{\mu}/dc$ obtained from magnetization measurements which agree reasonably well with our $M(0)$ values. Fitted parameters are given in Table II and the moment disturbances for two of the alloys are compared in Fig. 6. These $M(K)$ functions exhibit the same general behavior as those observed for Ni-Cu (Ref. 9) and Ni-Rh (Ref. 11), namely, there are forward direction peaks which become sharper with increasing Pt content. These correspond to inhomogeneous-moment distributions which may be described as ferromagnetic clusters in the critical concentration region. The observed $\mathfrak{M}(K)$ functions, on the other hand, show peaks in the forward direction in NiCu and NiRh but not in NiPt. We attribute this to the observed SRO in these systems. NiCu forms chemical clusters which enhance the moment response to a concentration fluctuation measured by $M(K)$. NiRh forms random alloys and is, therefore, unaffected by SRO. NiPt shows a preference for unlike near neighbors which damps out the moment disturbances. The latter is illustrated by comparison of Figs. 4 and 5.

The $M(K)$ functions presented were obtained with polarized neutrons and should be compared with the $T(K)$ functions that are obtained with unpolarized neutrons. If moment fluctuations are

associated with site-occupation fluctuations, then $T(K)$ is related to $M(K)$ by the Eq. (2.9) given by Marshall¹²:

$$T(K) = S(K)M(K)^2 + \dots$$

In Fig. 7 we compare the measured unpolarized-magnetic cross sections (data points) with the calculated cross sections (continuous curve) using Eq. (2.9) and a large difference is observed.

Differences of this kind were observed in Ni-Cr and Ni-V (Ref. 13) and were discussed in terms of the nonlinear terms due to n -site perturbations. However, nonlinear effects are not observed in the low-charge contrast systems NiCu and NiRh ($\Delta Z = 1$) and are therefore not expected to occur in the isoelectronic system Ni-Pt. The origin of this behavior must be attributed to some other effect. Since $M(K)$ describes the moment fluctuations associated with concentration fluctuations while $T(K)$ includes all moment-moment fluctuations, these results show that there are extra correlations between the moment fluctuations that are not associated with concentration fluctuations. We have not been able to establish the source of these extra correlations.

V. CHEMICAL-MAGNETIC ENVIRONMENT MODEL

Chemical environment effects are associated with charge transfer and are expected to be small and short ranged in this isoelectronic system. We have found, however, that the moment disturbances after correction for SRO effects are long ranged. Similar long-range moment disturbances were found in NiCu and NiRh and were explained with a local environment model⁹ which assumes that the moment on an Ni atom is a function not only of its chemical environment but also of the magnetic moments of the surrounding atoms. In this way long-range moment disturbances can be explained as the propagation of the magnetic perturbation on an Ni atom to its neighbors which in turn pass them to their own neighbors and so on.

In this model the moment on an Ni atom is assumed to be a function of the number of impurity nearest neighbors ν and of an exchange field produced by its neighbors. We have then that the moment on an Ni atom at site \vec{n} is

$$\mu_{\vec{n}} = F(h_{\vec{n}}, \nu_{\vec{n}}), \quad (5.1)$$

in which ν is the number of Pt nearest neighbors

$$\nu_{\vec{n}} = \sum_{\vec{\delta}} p_{\vec{n}, \vec{\delta}}, \quad (5.2)$$

and h is an exchange field given by

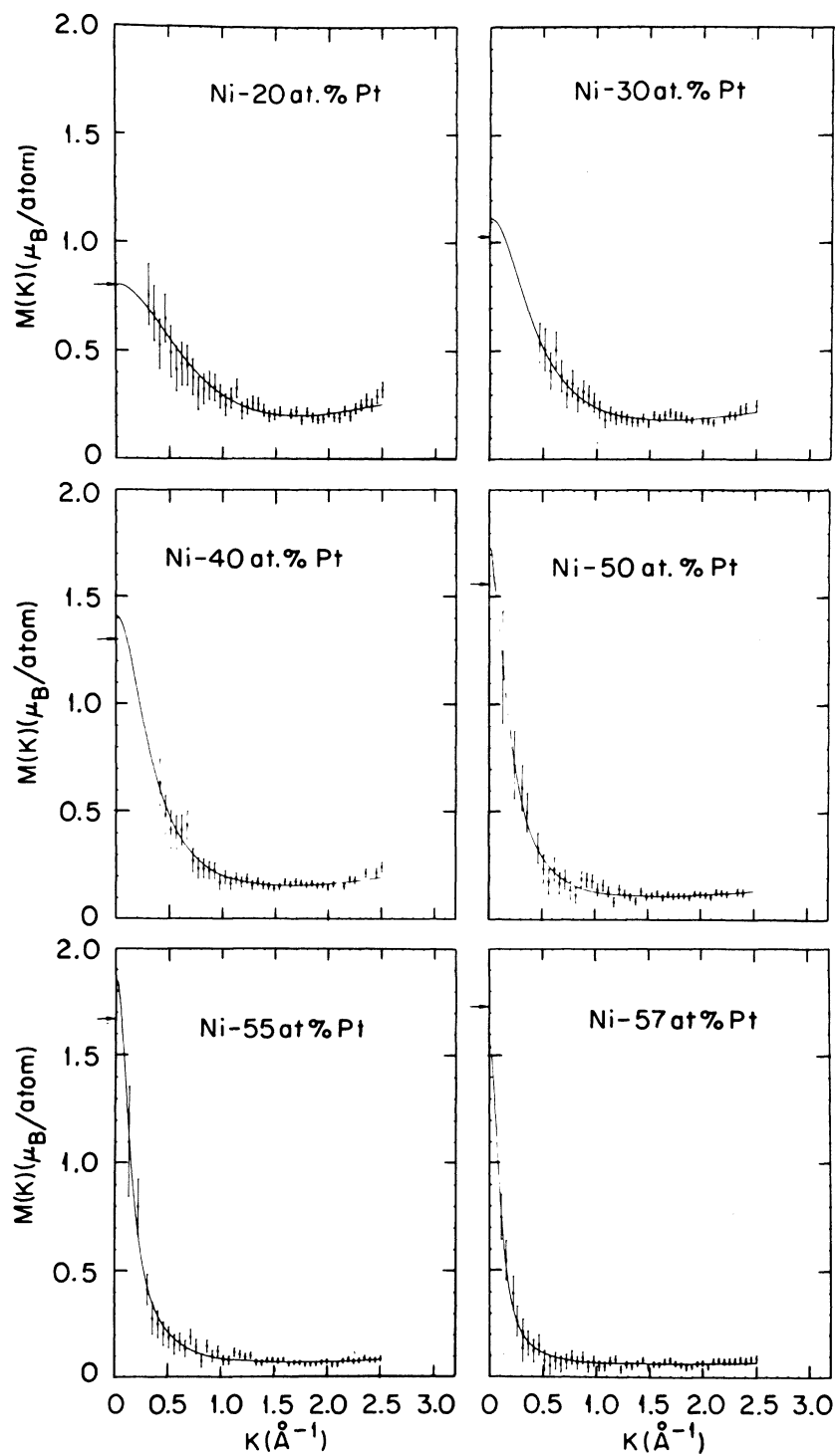


FIG. 5. NiPt moment disturbances. The arrows indicate values of $d\bar{\mu}/dc$ determined from magnetization measurements.

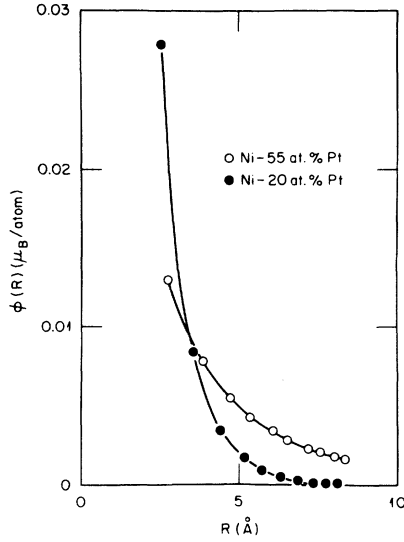


FIG. 6. Moment disturbances of Ni-55 at.% Pt and Ni-20 at.% Pt.

$$h_{\bar{n}} = \sum_{\bar{\delta}} J_{k\bar{l}} \mu_{\bar{n}+\bar{\delta}}^{\bar{l}}, \quad (5.3)$$

where the sums are over the $\bar{\delta}$ nearest neighbors of site \bar{n} , k and l denote the type of atoms occupying sites \bar{n} and $\bar{n} + \bar{\delta}$ and where

$$\mu_{\bar{n}} = (1 - p_{\bar{n}}) \mu_{\bar{n}}^{\text{Ni}} + p_{\bar{n}} \mu_{\bar{n}}^{\text{Pt}}. \quad (5.4)$$

If we assume that the Ni moment fluctuations are small, we can expand $\mu_{\bar{n}}^{\text{Ni}}$ about an effective field h_{eff} and $\langle \nu \rangle$:

$$\mu_{\bar{n}}^{\text{Ni}} = \langle \mu_{\text{Ni}} \rangle + \frac{\partial F}{\partial h} (h_{\bar{n}} - h_{\text{eff}}) + \frac{\partial F}{\partial \nu} (\nu_{\bar{n}} - \langle \nu \rangle), \quad (5.5)$$

where

$$\langle \mu_{\text{Ni}} \rangle = F(h_{\text{eff}}, \langle \nu \rangle). \quad (5.6)$$

The moment on a Pt atom also depends on its chemical and magnetic environment and should also be described in a manner analogous to Eq. (5.5). However, this introduces two additional parameters into the problem and seriously complicates the calculation of $M(K)$. We have therefore introduced the following approximation. We note that our direct results give $\bar{\mu}_{\text{Ni}} \approx 2\bar{\mu}_{\text{Pt}}$ at all concentrations. We assume that this also applies locally so that in any given environment an Ni atom would have twice the moment of a Pt atom in that same environment. Thus, $\mu_{\bar{n}}^{\text{Ni}} = 2\mu_{\bar{n}}^{\text{Pt}}$ and we need only evaluate the Ni moment fluctuations to calculate $M(K)$. For the random alloy, we obtain

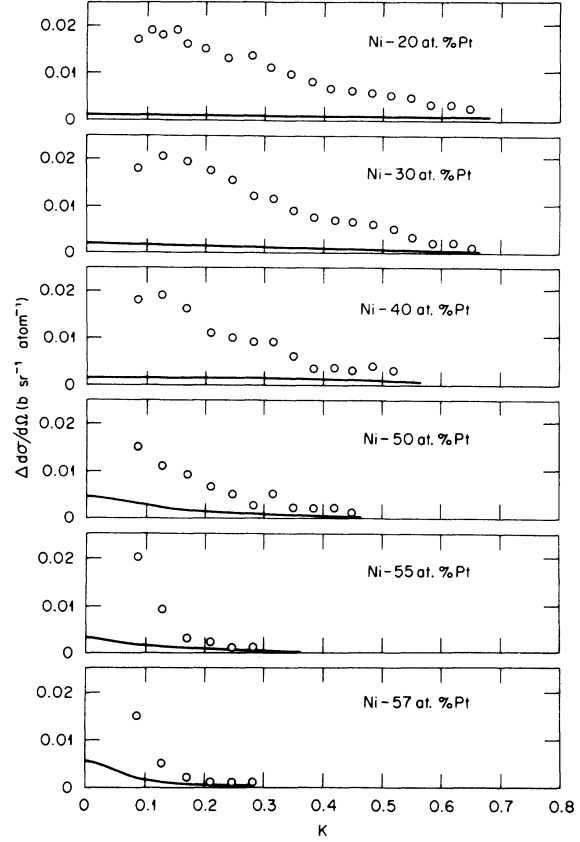


FIG. 7. Unpolarized magnetic cross section (points) and calculated cross section (continuous curve) using Eq. (2.9).

$$M(\vec{K}) = \bar{\mu}_{\text{Pt}} f_{\text{Pt}}(\vec{K}) - \bar{\mu}_{\text{Ni}} f_{\text{Ni}}(\vec{K}) + \left(1 - \frac{c}{2}\right) \frac{\mu_s}{\gamma} \left(\frac{1}{[1 - \Gamma \Phi_1(\vec{K})] B(\Gamma)} - 1 \right), \quad (5.7)$$

where the following definitions have been used:

$$\mu_s = \epsilon \bar{\mu}_{\text{Pt}} - \bar{\mu}_{\text{Ni}} + \rho z_1, \quad (5.8)$$

$$\gamma = 1 - c + \frac{1}{2} \epsilon c, \quad (5.9)$$

$$\epsilon = J_{\text{NiPt}} / J_{\text{NiNi}}, \quad (5.10)$$

$$\rho \Gamma = \gamma \partial F / \partial \nu, \quad (5.11)$$

$$\Gamma = \gamma z_1 J_{\text{NiNi}} \partial F / \partial h, \quad (5.12)$$

$$\Phi_1(K) = \frac{1}{z_1} \sum_{\bar{\delta}} e^{i\vec{K} \cdot \bar{\delta}}, \quad (5.13)$$

and

$$B(\Gamma) = \frac{1}{V} \int_{\text{FBZ}} d\vec{K} \frac{1}{1 - \Gamma \Phi_1(\vec{K})}, \quad (5.14)$$

where the integral is over the first Brillouin zone

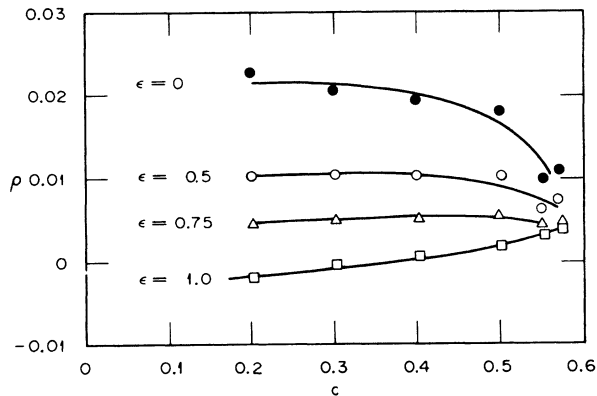


FIG. 8. Parameters ρ for different values of ϵ . In this figure and in Figs. 9–11 the continuous curves have no theoretical basis and are intended as a guide only.

(FBZ). Thus, $M(K)$ consists of a constant-moment difference term plus a K -dependent moment-disturbance term. Since $\Phi_1(K)$ is just the form factor of the first-neighbor shell normalized to unity at $K=0$, the K dependence of $M(K)$ is determined solely by the magnitude of the magnetic environment parameter Γ . The $M(K)$ data, corrected for the moment difference term and normalized to their $K=0$ values, can therefore be fitted to Eq. (5.7) with the single parameter Γ . Fitted Γ 's and the corresponding $B(\Gamma)$'s are then used in the $K=0$ limit to find μ_s using Eq. (5.7):

$$M(0) = -\bar{\mu}_{Ni} + \bar{\mu}_{Pt} + \left(1 - \frac{c}{2}\right) \frac{\mu_s}{\gamma} \left(\frac{1}{(1-\Gamma)B(\Gamma)} - 1 \right). \quad (5.15)$$

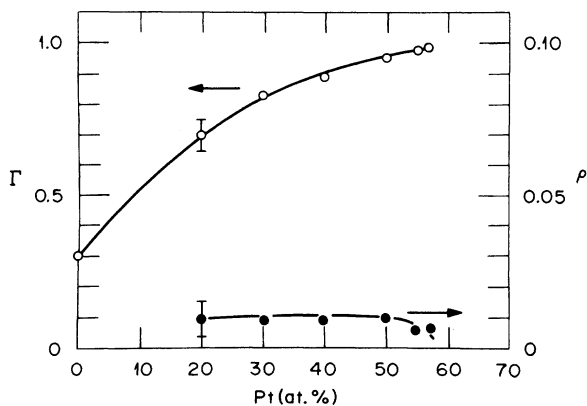


FIG. 9. Chemical and magnetic environment parameters for NiPt alloys ($\epsilon=0.56$).

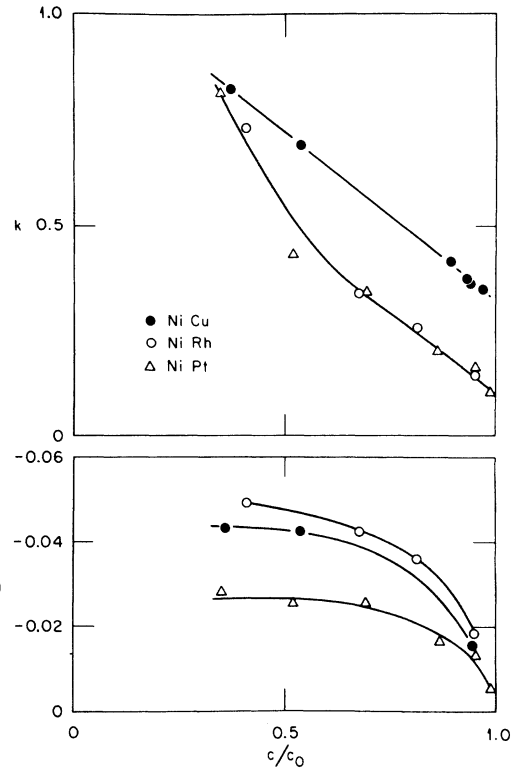


FIG. 10. Comparison of the inverse range parameter and nearest-neighbor moment disturbance of NiPt, NiRh, and NiCu.

The chemical environment parameter ρ can be determined from the values of μ_s using Eq. (5.8) but first we must estimate the ratio of exchange constants ϵ . The parameters ρ are given as a function of concentration in Fig. 8 for different values of ϵ . The value of ϵ calculated in terms of the Curie temperatures²⁰ is $\epsilon=0.56$. The values of the fitted Γ and of ρ (calculated with $\epsilon=0.56$) are shown in Fig. 9 where Γ at $c=0$ is an extrapolation of the NiCu results⁹ and corresponds to that of pure Ni ($\Gamma_0=0.305$). The magnetic parameter Γ describes the moment response to a change in the exchange field. This parameter increases with increasing Pt concentration or, more significantly, with decreasing average moment. This corresponds to the behavior expected for a saturating F versus h function. The chemical environment parameter ρ describes the moment response to a change in the number of Pt nearest neighbors. These parameters are very small as expected since Ni and Pt are isoelectronic. Most of the moment disturbances are clearly caused by the magnetic environment.

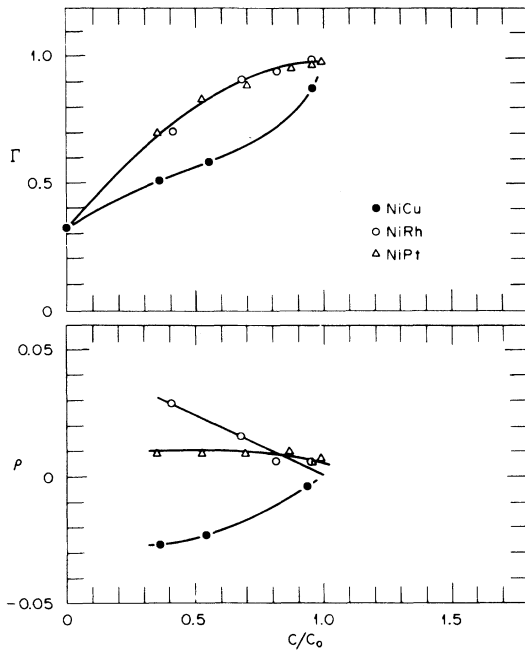


FIG. 11. Comparison of the magnetic and chemical environment parameter of NiPt, NiRh, and NiCu.

It is interesting to compare the results for this system with two other systems for which this model has been applied: NiRh (Ref. 11) and NiCu (Ref. 9). The three systems are compared in Figs. 10 and 11 for the inverse range parameter k , the first-neighbor moment disturbance $\phi(R_1)$, the magnetic environment parameter Γ , and the chemical environment parameter ρ against c/c_0 . The three systems show first-neighbor moment disturbances which decrease in magnitude as the impurity concentration is increased. In NiRh and NiPt there are magnetic moments on both the host and impurity atoms and they show good agreement for Γ and k . NiCu, with a non-magnetic impurity, shows different magnitudes for Γ and k values but with the same trend as for the NiPt and NiRh values. The main difference is in the values of the chemical environment parameters ρ , which are positive for NiRh and NiPt (assuming $\epsilon = 0.56$) and negative in NiCu. This agrees qualitatively with the charge transfer predicted by Van der Rest.²¹ The Ni d bands in NiRh and NiPt are higher in energy than those of Rh or Pt so the Ni loses electrons causing an increase of the Ni moment and positive ρ values. NiPt has $\Delta Z = 0$ and thus smaller ρ values than NiRh with $\Delta Z = 1$. On the other hand the charge transfer is toward Ni in NiCu causing a decrease of the Ni moment and negative ρ values.

VI. CONCLUSIONS

We have measured the average moments and the moment disturbances in six ferromagnetic Ni-Pt alloys. The results indicate that the average Ni moment decreases with Pt concentration while the Pt moment is about half that of Ni throughout our concentration range. Moment disturbance functions corresponding approximately to the random alloy have been obtained using Marshall's model, which assumes that moment disturbances are produced by concentration fluctuations, and they show inhomogeneous-moment distributions that can be described as ferromagnetic clusters.

These polycrystalline samples show a large amount of short-range order which affects the magnetic order of the system. The observed nuclear-magnetic correlation function shows a difference of the average moments and very little structure corresponding to a fairly homogeneous-moment distribution. The same correlation corrected for short-range order shows moment disturbances which increase in range with increasing Pt concentration. A comparison with NiRh and NiCu explains the apparent difference in the magnetization of these alloys. NiRh is a random alloy and its magnetic response is unaffected by short-range order. NiCu has a strong tendency to form chemical clusters and this favors the development of ferromagnetic clusters; NiPt tends to anticluster which in effect damps out the ferromagnetic clusters. An analysis of the data with a local environment model, which assumes that the moment on an Ni atom is a function of its nearest chemical environment as well as of the magnetic moments of the surrounding atoms, indicates that most of the moment disturbances are caused by the magnetic environment. A comparison of this system with ferromagnetic NiRh and NiCu systems, for which the onset of ferromagnetism has been explained as the alignment of the observed polarization clouds, shows agreement on the extent of the polarization clouds and on the range of the magnetic environment effects for NiPt and NiRh. Shorter ranges are found in NiCu. Both the host and the impurity are magnetic in NiPt and NiRh while in NiCu the impurity Cu is non-magnetic.

A comparison of the polarized and unpolarized neutron measurements shows that there are extra correlations between moment fluctuations that are not dependent on concentration fluctuations and cannot, therefore, be analyzed with Marshall's model.

Summarizing, there are long-range moment disturbances in ferromagnetic NiPt alloys that can be explained in terms of magnetic environment effects

and that are affected by the state of chemical short-range order of the system.

ACKNOWLEDGMENTS

The authors are grateful to R. H. Kernohan for helping with the magnetization measurements and

to H. R. Child for assistance with the computer programs. They also thank J. Sellers and A. Zulliger for their technical assistance during the experiments. This research was sponsored by the Division of Material Sciences U. S. Department of Energy under Contract No. W. 7405-eng-26 with the Union Carbide Corporation.

*Present address: IVIC, Centro de Fisica, APDO, 1827, Caracas, Venezuela.

¹E. C. Stoner, *Philos. Mag.* **15**, 1018 (1933).

²D. M. Edwards and E. P. Wohlfarth, *Proc. R. Soc. London A* **303**, 127 (1968).

³D. J. Gillespie and A. I. Schindler, in *Proceedings of the 17th Annual Conference on Magnetism and Magnetic Materials, Chicago, 1971* (AIP, New York, 1972), p. 461.

⁴H. L. Alberts, J. Beille, D. Bloch, and E. P. Wohlfarth, *Phys. Rev. B* **9**, 2233 (1974).

⁵J. Beille, D. Bloch, and M. J. Besnus, *J. Phys. F* **4**, 1275 (1974).

⁶F. Acker and R. Huguenin, *J. Magn. Magn. Mater.* **12**, 58 (1979).

⁷J. S. Kouvel and J. B. Comly, *Phys. Rev. Lett.* **24**, 598 (1970).

⁸T. J. Hicks, B. Rainford, J. S. Kouvel, and G. G. Low, *Phys. Rev. Lett.* **22**, 531 (1969).

⁹R. A. Medina and J. W. Cable, *Phys. Rev. B* **15**, 1539 (1977).

¹⁰W. C. Mueller and J. S. Kouvel, *Phys. Rev. B* **11**,

4552 (1975).

¹¹J. W. Cable, *Phys. Rev. B* **15**, 3477 (1977).

¹²W. Marshall, *J. Phys. C* **1**, 88 (1968).

¹³J. W. Cable and R. A. Medina, *Phys. Rev. B* **13**, 4868 (1976).

¹⁴J. M. Cowley, *Diffraction Physics* (North-Holland, Amsterdam, 1975), Chap. 12.

¹⁵J. W. Cable, R. E. Parra, and H. R. Child, *Solid State Commun.* **27**, 911 (1978).

¹⁶M. A. Krivoglaz, *Theory of X-Ray and Thermal Neutron Scattering by Real Crystals* (Plenum, New York, 1969).

¹⁷R. M. Moon, *Int. J. Magn.* **1**, 219 (1971).

¹⁸R. Maglic, T. O. Brun, G. P. Felcher, Y. K. Chang, and J. B. Ketterson, *J. Magn. Magn. Mater.* **9**, 318 (1978).

¹⁹J. B. Comly, T. M. Holden, and G. G. Low, *J. Phys. C* **1**, 458 (1968).

²⁰T. C. Pilkington, J. L. Artley, and F. T. Wooten, *J. Phys. Appl.* **35**, 3493 (1964).

²¹J. Van der Rest, *J. Phys. F* **7**, 1051 (1977).